DIFFERENTIAL MORPHOLOGY: MULTISCALE IMAGE DYNAMICS, MAX–MIN DIFFERENCE EQUATIONS, AND SLOPE TRANSFORMS

Petros Maragos

School of ECE, Georgia Institute of Technology, Atlanta, GA 30332–0250, USA

ABSTRACT

We develop 2D max–min difference equations that model the space dynamics of 2D morphological systems and some nonlinear signal transforms, called *slope transforms*, that can analyze these systems in a transform domain in a way conceptually analogous to the application of Fourier transforms to linear systems. Further, we discuss some nonlinear partial differential equations (PDEs) that model the evolution of multiscale morphological filters of the max–min type. These PDEs are related to the eikonal equation. Solutions of the eikonal PDE are proposed based on 2D min difference equations that can compute distance transforms. We view the analysis of the multiscale morphological PDEs and of the eikonal PDE solved via max–min equations as a unified area in nonlinear image processing which we call *differential morphology*. Its potential applications include distance-path finding, segmentation, gridless halftoning, and shape from shading.

1. INTRODUCTION

Morphological image processing is based on set- or lattice-theoretic concepts and a broad class of nonlinear signal operators, called morphological systems or filters. These are parallel and/or serial interconnections of morphological **dilations** $(x \oplus g)(v) = \bigvee_{u \in E} x(u) + g(v-u)$ or morphological **erosions** $(x \ominus g)(v) = \bigwedge_{v \in E} x(u) - g(u-v)$, where $\bigvee$ and $\bigwedge$ denote supremum and infimum, and $E = \mathbf{R}^d$ or $\mathbf{Z}^d$. Compositions of erosions and dilations yield two other useful morphological smoothing filters: the **opening** $x \circ g = (x \ominus g) \oplus g$ and **closing** $x \bullet g = (x \oplus g) \ominus g$.

Despite the wide applicability of morphological systems to image processing and computer vision, so far their analysis has lacked a transform domain. In this paper we present various analytic methods to determine the output and properties of these nonlinear systems in the spatial domain based on their *impulse response* or on *2D max-min difference equations* that describe the space dynamics of these systems. Further, to understand their behavior in a transform domain–the slope domain–we develop signal transforms, called *slope transforms*, whose properties and application to morphological systems has some striking conceptual similarities with Fourier transforms and their application to linear systems. We focus on multidimensional signal and systems; a similar work for 1D signals and systems can be found in Maragos [4, 5, 6].

In computer vision, several image analysis tasks related to physical phenomena have been successfully modeled via PDEs. Examples include shape from shading, optical flow, and modeling multiscale analysis via the heat equation. Multiscale signal analysis is a useful and often required framework for many tasks such as feature/object detection, motion detection, and multi-band frequency analysis. While the majority of such approaches used so far have been *linear*, a general understanding arises for the limitations or inability of linear systems to successfully model several image processing problems, and the need grows for developing nonlinear approaches. Brockett and Maragos [2] have developed some *nonlinear PDEs* to model the evolution of morphological image operators of the max–min type in scale-space. From a different viewpoint, multiscale filtered versions of binary images can be obtained via morphological distance transforms and can be modeled via similar ideas as in optic wave propagation governed by the eikonal PDE. The *eikonal equation* can be solved using distance transforms, which in turn can be implemented via 2D recursive max-min equations.

Thus, there is a close relationship between the morphological multiscale and eikonal PDEs, and the space-and-slope-domain analysis of morphological systems. The unifying theme is a collection of max-min differential/difference equations modeling the scale or space dynamics of morphological systems, and the slope transforms that can analyze these systems in a transform domain. We call the area of the multiscale morphological PDEs and the max-min difference equations used to solve the eikonal equation as *differential morphology*. Whereas classical morphological image processing is based on set and lattice theory, differential morphology offers calculus-based tools and some exciting connections to the physics of wave propagation.

2. MORPHOLOGICAL SYSTEMS

Assume signals $x(v)$ defined on a d-dimensional ($d = 1, 2, ..$) continuous ($E = \mathbf{R}^d$) or discrete domain ($E = \mathbf{Z}^d$) and whose range is any subset of $\overline{\mathbf{R}} = \mathbf{R} \cup \{-\infty, \infty\}$. In convex analysis [8] the nonlinear operation $\oplus$ is called 'maximal (or max-plus) convolution' and an operation closely related to $\ominus$ is the 'infimal (or min-plus) convolution' $(x \square g)(v) = \bigwedge_u x(u) + g(v-u)$.

We call a signal operator $\mathcal{D} : x \mapsto y = \mathcal{D}(x)$ a **dilation system** if it obeys the *supremum-of-sums superposi-*

This paper was written while the author was supported by the US National Science Foundation under Grant MIP–9396301.

0-8186-6950-0/94 $4.00 © 1994 IEEE

tion $\mathcal{D}[\bigvee_i c_i + x_i(v)] = \bigvee_i c_i + \mathcal{D}[x_i(v)]$. Two signals useful for analyzing morphological systems are the *zero impulse* μ and *zero step* λ, defined in the 1D case $v = t$ as

$$\mu(t) \triangleq \begin{cases} 0, & t = 0 \\ -\infty, & t \neq 0 \end{cases} \quad , \quad \lambda(t) \triangleq \begin{cases} 0, & t \geq 0 \\ -\infty, & t < 0 \end{cases}$$

and in the $d \geq 2$ case as $\mu(v) = \sum_{i=1}^{d} \mu(v_i)$ and $\lambda(v) = \sum_{i=1}^{d} \lambda(v_i)$. For example, a signal can be represented as a sup of weighted impulses: $x(v) = \bigvee_u x(u) + \mu(v-u)$. If $g(v) = \mathcal{D}[\mu(v)]$ is the system's **impulse response**, we find [5] that a **dilation shift-invariant (DSI)** system is equivalent to a max-plus convolution of the input with its impulse response:

$$\mathcal{D} \text{ is DSI} \iff \mathcal{D}(x) = x \oplus g, \quad g \triangleq \mathcal{D}(\mu)$$

Thus, a DSI system is uniquely determined in the spatial domain by its impulse response, which also controls its causality and stability [4, 5].

Operators $\mathcal{E} : x \mapsto y = \mathcal{E}(x)$ that are shift-invariant and obey an infimum-of-sums superposition are called herein *erosion shift-invariant (ESI)* systems. These are equivalent to a min-plus convolution, because $\mathcal{E}$ is ESI iff $\mathcal{E}(x) = x \square f$, where $f = \mathcal{E}(-\mu)$ is their impulse response.

To describe the space dynamics of discrete ESI systems we consider the 2D **min-plus difference equations**

$$\begin{aligned} y[n,m] \quad = \quad & \left(\bigwedge_{(k,j) \in M_o} a_{kj} + y[n-k, m-j] \right) \\ & \wedge \left(\bigwedge_{(p,q) \in M_i} b_{pq} + x[n-p, m-q] \right) \end{aligned} \tag{1}$$

The masks M_o, M_i are pixel coordinate sets that determine which output and input samples will be added with constants to form the current output sample. Similarly, the dynamics of DSI systems can be described by max-plus difference equations as in (1) but with $\bigwedge$ replaced by $\bigvee$. For erosion (resp. dilation) systems the useful information in a signal x exists only at points v where $x(v) < +\infty$ (resp. $x(v) > -\infty$). The vast majority of discrete max/min-plus convolutions $\oplus$,$\ominus$ used in applications employs a finite structuring element, and they can be modeled by the above max/min difference equations by ignoring the recursive part (i.e., if all $a_{kj} = \pm\infty$). The only exception has been recursive erosions which can generate the distance transform of binary images [1].

To create a **transform domain** for morphological systems, we first note that the hyperplanes $x(v) = \alpha \cdot v + b$ are *eigenfunctions* of any DSI system $\mathcal{D}$ or ESI system $\mathcal{E}$ because

$$\mathcal{D}[\alpha \cdot v + b] = \alpha \cdot v + b + G(\alpha) \quad , \quad G(\alpha) \triangleq \bigvee_v g(v) - \alpha \cdot v$$

$$\mathcal{E}[\alpha \cdot v + b] = \alpha \cdot v + b + F(\alpha) \quad , \quad F(\alpha) \triangleq \bigwedge_v f(v) - \alpha \cdot v$$

where $\alpha = (\alpha_1, ..., \alpha_d) \in \mathbf{R}^d$ and $\alpha \cdot v = \sum_{i=1}^{d} \alpha_i v_i$. We call the corresponding eigenvalues $G(\alpha)$ and $F(\alpha)$ the **slope response** of the DSI and ESI system. It measures the amount of shift in the intercept of the input hyperplanes with slope vector α. It is also conceptually similar to the frequency response of linear systems.

3. SLOPE TRANSFORMS

Viewing the slope response as a signal transform with variable the slope vector α, we define for any signal $x(v)$ its **upper slope transform** as the function $X_\vee : \mathbf{R}^d \to \overline{\mathbf{R}}$ and as **lower slope transform**[1] the function $X_\wedge$:

$$X_\vee(\alpha) \triangleq \bigvee_{v \in E} x(v) - \alpha \cdot v \quad , \quad X_\wedge(\alpha) \triangleq \bigwedge_{v \in E} x(v) - \alpha \cdot v$$

In general, $x(v)$ is covered from above by all the hyperplanes $X_\vee(\alpha) + \alpha \cdot v$ whose infimum creates an *upper envelope* $\hat{x}(v)$ and is covered from below by planes $X_\wedge(\alpha) + \alpha \cdot v$ whose supremum creates the *lower envelope* $\check{x}(v)$:

$$\hat{x}(v) \triangleq \bigwedge_{\alpha \in \mathbf{R}^d} X_\vee(\alpha) + \alpha \cdot v \quad , \quad \check{x}(v) \triangleq \bigvee_{\alpha \in \mathbf{R}^d} X_\wedge(\alpha) + \alpha \cdot v$$

We view the signals $\hat{x}(v)$ and $\check{x}(v)$ as the 'inverse' upper and lower slope transform of $x(v)$, respectively.

Theorem 1. *For any signal* $x : \mathbf{R}^d \to \overline{\mathbf{R}}$, *(a)* $X_\vee(\alpha)$ *and* $\check{x}(v)$ *are convex, whereas* $X_\wedge(\alpha)$ *and* $\hat{x}(v)$ *are concave. (b) For all* v, $\check{x}(v) \leq x(v) \leq \hat{x}(v)$. *(c) At any point* v, $\hat{x}(v) = x(v)$ *iff*

$$x(v) \geq \frac{px(v-qu) + qx(v+pu)}{p+q} \quad \forall p, q > 0, \quad \forall ||u|| = 1. \tag{2}$$

At any v, $x(v) = \check{x}(v)$ *iff the* $\geq$ *sign in* (2) *is replaced by* $\leq$. *(d)* $\hat{x}(v) = x(v)$ *for all* v *if* x *is concave, and* $\check{x} = x$ *if* x *is convex. (e)* $\hat{x}$ *is the smallest concave upper envelope of* x, *and* $\check{x}$ *is the greatest convex lower envelope of* x.

Tables I and II list several properties and examples of the 2D upper slope transform. The most striking is that (dilation) max-plus convolution in the time/space domain corresponds to addition in the slope domain. Note the analogy with linear systems where linearly convolving two signals in space corresponds to multiplying their Fourier transforms.

Whatever we discussed for upper slope transforms also applies to the lower slope transform, the only differences being the interchange of suprema with infima, concave with convex, and dilation with erosion.

For **differentiable** signals, the maximization or minimization of the intercept $x(v) - \alpha \cdot v$ involved in both slope transforms can also be done, for a fixed α, by finding its value at the stationary point v^* such that $\nabla x(v^*) = \alpha$. At the point $(v^*, x(v^*))$ the hyperplane becomes tangent to the graph. This extreme value of the intercept (as a function of the slope α) is the *Legendre transform* of the signal x:

$$X_L(\alpha) \triangleq x\left((\nabla x)^{-1}(\alpha)\right) - \alpha \cdot (\nabla x)^{-1}(\alpha)$$

It is extensively used in mathematical physics. If the signal $x(v)$ is concave or convex and has an invertible gradient, its Legendre transform is single-valued and equal (over the slope regions it is defined) to the upper or lower transform;

[1] In convex analysis [8], given a convex function h there uniquely corresponds another convex function $h^*(\alpha) = \bigvee_v \alpha \cdot v - h(v)$ called the *conjugate* of h. The lower slope transform of h and its conjugate function are closely related since $h^*(\alpha) = -H_\wedge(\alpha)$.

e.g., see the last four examples in Table II. If a differentiable signal is neither convex nor concave or if it does not have an invertible gradient, the Legendre transform is multi-valued; i.e., $X_L(\alpha)$ is a set of real numbers for each α. This multi-valued Legendre transform is defined for the 1D case in [3] as a 'slope transform' and is expressed via stationary points; i.e., $X_L(\alpha) = \{x(t^*) - \alpha t^* : x(t^*) = \alpha\}$. Its properties in [3] are similar to the properties of the upper/lower slope transform, but there are also some important differences (see [5, 6]).

4. MAX–MIN EQUATIONS, SLOPE FILTERS, AND DISTANCE TRANSFORMS

We view (1) as a 2D discrete nonlinear system $x \mapsto y$, and we assume boundary conditions of value $+\infty$ and of a shape (dependent on M_o and the scanning order) appropriate so that the difference equation is an ESI system recursively computable. The nonrecursive part of this equation represents a min-plus convolution $\square$ of the input array $x[n,m]$ with the 2D finite-support structuring function $b[n,m] = b_{nm}$. Henceforth, we focus only on the recursive min version of (1) by setting $b_{pq} = +\infty$ except from $b(0,0) = 0$. If $f[n,m] = \mathcal{E}(-\mu[n,m])$ is the impulse response of the corresponding ESI system $\mathcal{E}$, then $y = x \square f$. Finding a closed-formula expression for f is generally not possible. However, we can first find the slope response F and then, via inverse lower slope transform, find the impulse response f or its envelope $\check{f}$. Applying lower slope transforms to both sides of (1) and using the fact that $Y_\wedge(\alpha) = F(\alpha) + X_\wedge(\alpha)$ yields

$$F(\alpha) = \begin{cases} 0, & \alpha \in R = \{\alpha : \alpha \cdot (k,j) \le a_{kj}\ \forall (k,j) \in M_o\} \\ -\infty, & \alpha \notin R \end{cases} \tag{3}$$

Thus the system acts as a 2D *slope filter* passing all input lower slopes α in the planar region R unchanged and rejecting the rest. R is a convex region determined by the inequalities $k\alpha_1 + j\alpha_2 \le a_{kj}$. The inverse slope transform on F yields the lower envelope $\check{f}$ of the impulse response f. Over short-scale periods f has the shape induced by the sequence $\{a_{kj}\}$. But over scales much longer than the size of the coefficient mask M_o, f behaves like its lower envelope $\check{f}$. Together F and $\check{f}$ can describe the long-scale dynamics of the system. In addition, if f is a plane, then the above analysis is also exact for the short-scale behavior.

Examples: Let $M_o = \{(0,1),(0,1),(1,1),(-1,1)\}$ and

$$\begin{aligned} y_1[n,m] &= \min(y_1[n-1,m] + a_{10}, y_1[n,m-1] + a_{01}, \\ & y_1[n-1,m-1] + a_{11}, y_1[n+1,m-1] + a_{-11}, x[n,m]) \end{aligned} \tag{4}$$

Let $a_{10} = a_{01} = 1$ and $a_{11} = a_{-11} = +\infty$. Assuming $+\infty$ boundary conditions and a bottom-left to top-right scanning order, the impulse response (found by induction) is $f_1[n,m] = a_{10}n + a_{01}m - \lambda[n,m]$ and the slope response is $F_1(\alpha_1,\alpha_2) = \lambda(a_{10} - \alpha_1, a_{01} - \alpha_2)$. Thus this system acts as a 2D lowpass slope filter passing all input lower slopes $\alpha_1 \le a_{10}$ and $\alpha_2 \le a_{01}$, and rejecting the rest. This example demonstrates that when ESI systems described by min difference equations have a recursive part, their impulse response has infinite support. The min equation in this example is used to compute the first pass $y_1 = x \square f_1$ of the distance transform for the **city-block distance** (using the 5-pixel diamond as the unit disk) of a binary image x. The distance transform y is completed via a second pass $y = y_1 \square f_2$, where $f_2[n,m] = f_1[-n,-m]$, or equivalently as $y = y_1 \wedge y_2$ where $y_2 = x \square f_2$. Thus the distance transform $x \mapsto y$ is an ESI system with impulse response $f = f_1 \wedge f_2$ and slope response $F = F_1 \wedge F_2$, where $f[n,m] = |n| + |m|$, and $F(\alpha) = 0$ if $||\alpha||_\infty \le 1$ and $-\infty$ else. Thus F is the indicator function of the unit square.

Let now $a_{10} = a_{01} = 3$ and $a_{11} = a_{-11} = 4$. Then, running the min equation in a bottom-left to top-right scan yields the first pass y_1 of the **chamfer (3,4) distance** algorithm [1]. The slope response of the complete distance computation system is the indicator function of the octagon shown in Fig. 1a. Thus, in general, the 2D discrete distance transforms are ESI systems whose slope responses are indicator functions of symmetric polygonal approximations to the disk in the slope plane and whose impulse responses are approximations to space cones. They are 2D ideal-cutoff bandpass slope filters.

If their coefficients are spatially-invariant, the min difference equations can produce unweighted distance transforms whose gradient magnitude is fixed. In computer vision, there are several applications of gray-weighted distance transforms whose gradient magnitude varies locally. We examined 2D min equations with spatially-varying coefficients that can generate such gray-weighted distances. One approach (see Fig. 1(c) for a simulated example) is to vary the coefficients proportionally to the local image intensities with proportionality constants equal to the weights of the discrete 2D metric used. Such gray-weighted distance transforms are approximate solutions [10] to the eikonal equation modeling optic wave propagation. Solving the eikonal equation has applications in recovering 3D shape from shading [10] and in gridless image halftoning [7]; see Fig. 1d.

5. MULTISCALE MORPHOLOGICAL PDES

Most of the work in multiscale image analysis involves obtaining the multiscale linear convolutions $\gamma(x,s) = f(x) * G_s(x)$ of the original image $f(x)$ with a Gaussian $G_s(x)$ whose variance is proportional to scale s. The popularity of this approach is due to its linearity and the fact that the multiscale function γ can be generated from the isotropic heat **diffusion equation** $\partial\gamma/\partial s = \partial^2\gamma/\partial x^2$. The big disadvantage of the Gaussian multiscale approach is the fact that linear smoothers blur and shift important image features, e.g. edges. In contrast, morphological smoothing filters, such as openings and closings, can smooth while preserving important image features and correspond to simple filtering operations. See Fig. 2 for examples. So far the implementations of multiscale morphological filtering have been discrete. Motivated by the renewed interest in analog systems, Brockett & Maragos [2] developed **nonlinear PDEs** that represent dynamical systems modeling multiscale morphological erosions/dilations and openings/closings. We shall limit our discussion to the PDEs generating multiscale erosions and dilations.

The **multiscale dilation** and **erosion** of f by g at scale

s are defined as the space-scale functions

$$u(x,s) \triangleq f \oplus g_s(x) \quad ; \quad v(x,s) \triangleq f \ominus g_s(x)$$

where $g_s : sB \rightarrow \mathbf{R}$ is a multiscale version of the structuring function g defined by $g_s(x) = sg(x/s)$, $s > 0$, with $sB = \{sb : b \in B\}$. The function g_s has the same shape as g but both its domain and range are scaled by a factor s. Figure 3 shows examples of such scale-space functions v and u. Given a 1D signal $f : \mathbf{R} \rightarrow \mathbf{R}$ and a 'flat' $g : [-1,1] \rightarrow \{0\}$, the PDEs generating the multiscale flat dilations and erosion of f by g are [2]:

$$\textbf{Dilation PDE:} \quad \frac{\partial u}{\partial s} = \left|\frac{\partial u}{\partial x}\right| \qquad \textbf{Erosion:} \quad \frac{\partial v}{\partial s} = -\left|\frac{\partial v}{\partial x}\right| .$$

These simple but nonlinear PDEs are satisfied at points (x,s) where the data are smooth, i.e., the partial derivatives $\partial u/\partial x$ and $\partial v/\partial x$ exist. Starting from a continuous f, the multiscale functions u and v remain continuous at all x and s. However, even if f is differentiable, as the scale s increases the multiscale erosions/dilations can create discontinuities in their derivatives $\partial/\partial x$; then these derivatives and the generator PDEs have to be interpreted correctly at such points according to the specific case. To solve this problem we can replace the conventional derivatives with 'morphological derivatives'; see [2] for details.

There exist similar nonlinear PDEs for the multiscale dilation of 2D signals $f(x,y)$ by concave functions $g : B \rightarrow \mathbf{R}$. The only difference now is that the shapes of g and its support B affect the form of the PDE. For example, if B is the unit disk and $g(x,y) = \sqrt{1-x^2-y^2}$ is the upper surface of the unit sphere, then the multiscale dilation function $u(x,y,s) = f(x,y) \oplus g_s(x,y)$ satisfies the PDE

$$\frac{\partial u}{\partial s} = \sqrt{1 + \left|\frac{\partial u}{\partial x}\right|^2 + \left|\frac{\partial u}{\partial y}\right|^2} = \sqrt{1 + ||\nabla u||^2} \qquad (5)$$

These PDEs suggest new ways to view and implement morphological multiscale filtering that avoid the shape discretization effects inherent in all discrete implementations [9].

6. EIKONAL PDE AND APPLICATIONS

In geometrical optics it is well-known that, the level sets of a 2D eikonal function $u(x,y)$, i.e., the solution to the **eikonal equation** $||\nabla u|| = n(x,y)$ are the constant-phase wavefronts of an electromagnetic wave propagating in medium of refractive index n. The eikonal equation is closely related to the multiscale morphological PDEs where the infinitesimal changes along the scale direction were expressed as functions of the spatial gradient magnitude; see (5). In a homogeneous medium, n is constant. If $n \equiv 1$, the wavefronts can be obtained from the multiscale dilations of the initial front by disks whose radii are proportional to the time of propagation. Thus *multiscale dilations by disks/spheres can implement Huygen's envelope construction.* See [9] for related discussion. Given this exciting connection between optical wave propagation and multiscale dilations in homogeneous media, we conjecture that it might also be possible in heterogeneous media to find the wavefronts as multiscale dilations by spacially-varying structuring elements. This is related to computing gray-weighted distance transforms, which in turn leads to the following applications:

One envisioned application is *shape from shading* where the height $z(x,y)$ of a Lambertian image surface can be found [10] as a solution of the PDE $||\nabla z|| = \sqrt{I^{-2}-1}$, and I is the intensity image. Another interesting application is *gridless image halftoning* where, inspired by the paradigm in [7], we attempt to solve the PDE $||\nabla u(x,y)|| = \text{const} - I(x,y)$ and create binary *gridless* halftone images that are the union of the level sets of the eikonal function $u(x,y)$. The goal here is to solve the eikonal PDE with an index $n(x,y)$ that is pixelwise controlled by the original gray-level image $I(x,y)$. An approximate solution [10] is the gray-weighted distance transform, which can be implented via shift-varying 2D min-plus equations, as discussed in Section 4. Fig. 1d shows that the isolevel contours of the distance transform (which we simulated as a solution of the halftoning eikonal PDE) provide a promising gridless halftoning approach.

7. REFERENCES

[1] G. Borgefors, "Distance Transformations in Digital Images", *Comp. Vision, Graphics, Image Process.*, 34, 344–371, 1986.

[2] R. W. Brockett and P. Maragos, "Evolution Equations for Continuous-Scale Morphological Filtering", *IEEE Trans. on Signal Processing*, Dec. 1994.

[3] L. Dorst and R. van den Boomgaard, "An Analytical Theory of Mathematical Morphology", *Proc. 1st Int'l Workshop on Math. Morphology and its Application to Signal Processing*, Barcelona, Spain, May 1993.

[4] P. Maragos, "Max-Min Difference Equations and Recursive Morphological Systems", *Proc. 1st Int'l Workshop on Math. Morphology and its Application to Signal Processing*, Barcelona, Spain, May 1993.

[5] P. Maragos, "Morphological Systems: Slope Transforms and Max–Min Difference and Differential Equations", *Signal Processing*, Sep. 1994.

[6] P. Maragos, "Slope Transforms: Theory and Application to Nonlinear Signal Processing", *Tech. Report 93–1*, DSP Lab, Georgia Inst. Tech., 1993.

[7] Y. Pnueli and A. M. Bruckstein, "Gridless Halftoning: A Reincarnation of the Old Method", CIS Report #9323, Technion, Israel, Oct. 1993.

[8] R. T. Rockafellar, *Convex Analysis*, Princeton Univ. Press, Princeton, 1972.

[9] G. Sapiro R. Kimmel, D. Shaked, B, Kimia, and A. Bruckstein, "Implementing Continuous-scale Morphology via Curve Evolution", *Pattern Recognition*, 26(9), pp. 1363–1372, 1993.

[10] P.W. Verbeek and B.J.H. Verwer, "Shading from shape, the eikonal equation solved by grey-weighted distance transform", *Pattern Recogn. Lett.*, 11:618–690, 1990.

TABLE I: Properties of 2D Slope Transform

Signal: $x(v)$ *	Transform: $X_\vee(\alpha)$ *
$\bigvee_i c_i + x_i(v)$	$\bigvee_i c_i + X_i(\alpha)$
$x(v - v_0)$	$X(\alpha) - \alpha \cdot v_0$
$x(v) + \alpha_0 \cdot v$	$X(\alpha - \alpha_0)$
$x(rv),\ \ r \in \mathbf{R}$	$X(\alpha/r)$
$rx(v)\ ,\ r > 0$	$rX(\alpha/r)$
$x(v) \oplus y(v)$	$X(\alpha) + Y(\alpha)$
$\bigvee_u x(u) + y(v+u)$	$X(-\alpha) + Y(\alpha)$
$x(v) \le y(v)\ \ \forall v$	$X(\alpha) \le Y(\alpha)\ \ \forall \alpha$
$y(v) = \begin{cases} x(v), & \|\|v\|\|_p \le r \\ -\infty, & \|\|v\|\|_p > r \end{cases}$	$Y(\alpha) = X(\alpha) \square r\|\|\alpha\|\|_q$ $1/p + 1/q = 1$
* $v = (v_1, v_2) \in \mathbf{R}^2$	$\alpha = (\alpha_1, \alpha_2) \in \mathbf{R}^2$

TABLE II: Examples of 2D Slope Transforms

Signal: $x(v)$	Transform: $X_\vee(\alpha)$
$\alpha_0 \cdot v$	$-\mu(\alpha - \alpha_0)$
$\alpha_0 \cdot v + \lambda(v)$	$-\lambda(\alpha - \alpha_0)$
$\mu(v - v_0)$	$-\alpha \cdot v_0$
$\lambda(v - v_0)$	$-\alpha \cdot v_0 - \lambda(\alpha)$
$\begin{cases} 0, & \|\|v\|\|_p \le r \\ -\infty, & \|\|v\|\|_p > r \end{cases}, p \ge 1$	$r\|\|\alpha\|\|_q, \quad \frac{1}{p} + \frac{1}{q} = 1$
$-\alpha_0 \|\|v\|\|_p, \quad \alpha_0 > 0$	$\begin{cases} 0, & \|\|\alpha\|\|_q \le \alpha_0 \\ +\infty, & \|\|\alpha\|\|_q > \alpha_0 \end{cases}$
$\sqrt{1 - v_1^2 - v_2^2},\ \ v_1^2 + v_2^2 \le 1$	$\sqrt{1 + \alpha_1^2 + \alpha_2^2}$
$-(v_1^2 + v_2^2)/2$	$(\alpha_1^2 + \alpha_2^2)/2$
$-(\|v_1\|^p + \|v_2\|^p)/p\ \ ,\ p > 1$	$(\|\alpha_1\|^q + \|\alpha_2\|^q)/q$
$\exp(v_1 + v_2)$	$\alpha_1\alpha_2 - \sum_{i=1}^{2} \alpha_i \log \alpha_i$

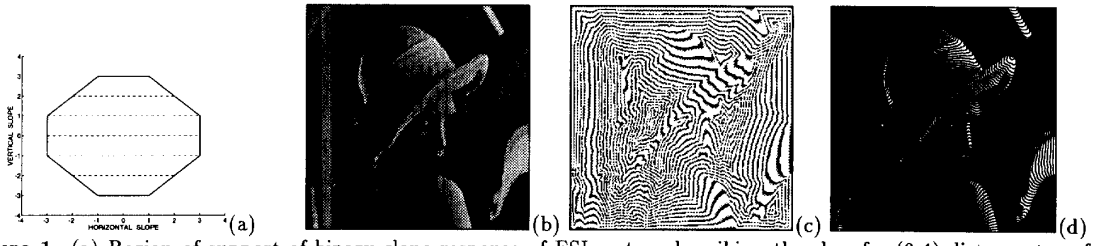

(a) (b) (c) (d)

Figure 1. (a) Region of support of binary slope response of ESI system describing the chamfer (3,4) distance transform. (b) Original gray image x. (c) Gray-weighted distance transform of x w.r.t. the (3,4) metric, displayed modulo 700. (d) Isolevel contour lines of the gray-weighted distance transform in (c) providing a gridless halftoning of the image x.

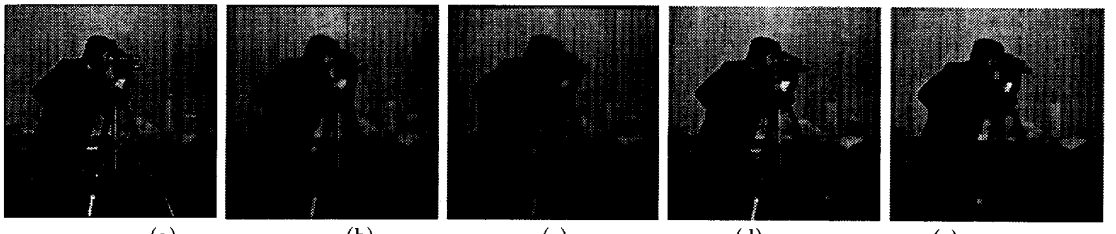

(a) (b) (c) (d) (e)

Figure 2. (a) Original image. Smoothing at scale=2,4 via: (b,c) Gaussian convolution, (d,e) clos-opening by a square.

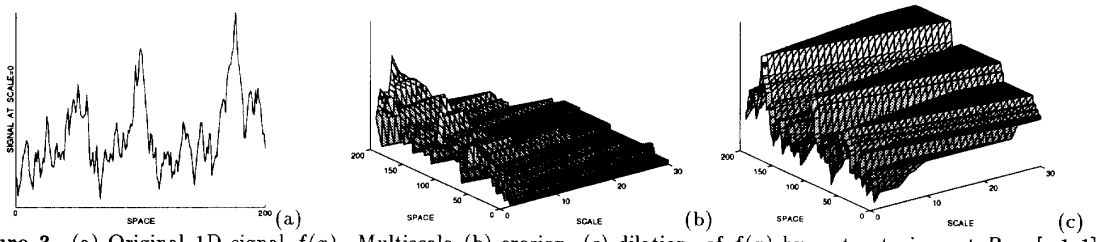

(a) (b) (c)

Figure 3. (a) Original 1D signal $f(x)$. Multiscale (b) erosion, (c) dilation, of $f(x)$ by a structuring set $B = [-1, 1]$ for scales $s = [0, 30]$.